

Edge Effects in Moderately Thick Plates under Creep-Damage Conditions

J. Altenbach, H. Altenbach and K. Naumenko

Dedicated to the memory of Prof. F.P.J. Rimrott (1927 - 2003).

The late F.P.J. Rimrott has published during his scientific life more than 200 refereed articles and conference papers. Various papers among them were devoted to the creep and plasticity analysis in metallic thin-walled structural elements mostly published in the period from 1958 till 1964. With regard to this early period below we discuss finite element solutions for moderately thick plates under creep-damage conditions based on shell and solid type finite elements. The results illustrate the time-dependent stress redistributions in the edge zones. We show that the transverse normal and shear stresses may have a significant influence on the damage evolution and must be considered in numerical lifetime estimations.

1 Introduction

In many applications engineering structures (beams, plates, pipes, pipe bends, etc.) operate at elevated temperatures. Under such conditions the behavior of metals and alloys is primarily determined by irreversible time-dependent creep and material deterioration processes. In order to estimate the long-term behavior it is important to understand the mechanisms of the time-dependent stress redistribution and damage growth, particularly in the zones of nozzles, pipe connections and welds.

The widely used approach in modelling the creep-damage behavior is the continuum damage mechanics, which proposes constitutive equations for the creep strain rate tensor, evolution equations for damage, hardening and other variables, and states nonlinear initial-boundary value problems in order to perform a structural analysis, e.g. Hayhurst (2001). With the progress in both the material science and the continuum mechanics, many new constitutive models have been developed which include physically motivated state variables. They are able to consider different effects in material behavior such as the damage induced anisotropy, the stress state dependence of damage evolution, etc. These models can be incorporated into a commercial finite-element code in order to analyze time-dependent deformations and stresses in thin-walled structures under a specific mechanical loading.

As usual, an important step is to select a structural mechanics model and to specify the type of finite elements. One way is the "three-dimensional approach" which is based on three-dimensional balance equations. This approach seems more preferable for creep-damage analysis since the existing constitutive models of creep-damage are developed with respect to the Cauchy stress and strain (rate) tensors and the proposed measures of damage (scalars or tensors of different rank) are defined in the three-dimensional space. Another way is the use of the classical two-dimensional structural mechanics equations of beams, plates and shells and the balance equations formulated in terms of force and moment tensors. This approach often find application because of simplicity of model creation, smaller effort in solving non-linear initial-boundary value problems of creep, and easily interpretable results. Different types of finite elements which are developed for the analysis of structures based on these two approaches are discussed, e.g., in Wriggers (2001).

The aim of this paper is to compare the long-term predictions based on the three-dimensional approach and a two-dimensional plate model and to discuss the possibilities and limitations of each approach in connection with the creep-damage analysis. In the first part, we summarize the basic features of creep behavior in metals and alloys, introduce the widely used Kachanov-Rabotnov-Leckie-Hayhurst material model Leckie and Hayhurst (1977) and demonstrate the description possibilities for stress states which are typical for beams, plates and shells. In the second part, we discuss the quasi-static initial-boundary value problems of creep-damage. Finally, we use the ANSYS finite element code in order to simulate the time-dependent behavior of a transversely loaded plate under creep-damage conditions. Based on the numerical example for a transversely loaded moderately thick square plate with two clamped parallel edges and two simply supported parallel edges we make conclusions regarding the realization of clamped edge boundary condition as well as the applicability of the shell and the solid type finite elements to the creep-damage analysis of engineering structures.

2 Creep-Damage Behavior and Basic Constitutive and Evolution Equations

Creep-damage behavior of polycrystalline metals and alloys is a phenomenon accompanied by different microstructural changes. It is known from material science that for moderate stresses (below the yield limit) and elevated temperatures (above $0.4T_m$ with T_m as the temperature at the melting point) the steady creep process is controlled by the climb plus glide dislocation mechanism Frost and Ashby (1982). The dependence of the creep strain rate on the applied stress can be described by the power law function¹. For multi-axial stress states the deviatoric part of the stress tensor and the von Mises equivalent stress are used to describe the deformation process. In addition to irreversible strains, material deterioration processes occur and lead to accelerated creep and final fracture. For polycrystalline materials, tertiary creep is accompanied by the nucleation and the growth of micro-voids on grain boundaries. The initially existing micro-voids have a negligible influence on the strain rate. As their number and size increase with time, they weaken the material providing the decrease in the load-bearing cross section. The nucleation kinetics can be related to the local grain boundary deformation as well as to the stress state characterized by the combination of the maximum tensile stress and the von Mises equivalent stress. The ratio between both stresses responsible for the damage process is different for different materials. The coalescence of cavities leads to the propagation of oriented micro-cracks and to final fracture. The cavities and micro-cracks nucleate on grain boundaries having different orientations. The significant influence of the damage induced anisotropy can be observed on the last stage before the creep rupture El-Magd et al. (1996).

The commonly used phenomenological model characterizes the secondary creep rate by the power law stress function and includes the effect of tertiary creep by means of the single scalar valued damage parameter Leckie and Hayhurst (1977). It can be presented as follows

$$\dot{\boldsymbol{\epsilon}}^{cr} = \frac{3}{2} a \left(\frac{\sigma_{vM}}{1 - \omega} \right)^n \frac{\mathbf{s}}{\sigma_{vM}}, \quad \dot{\omega} = b \frac{[\alpha \sigma_T + \beta \sigma_m + (1 - \alpha - \beta) \sigma_{vM}]^k}{(1 - \omega)^l} \quad (1)$$

with

$$\sigma_{vM} = \sqrt{\frac{3}{2} \mathbf{s} \cdot \mathbf{s}}, \quad \sigma_m = \frac{1}{3} \text{tr} \boldsymbol{\sigma}, \quad \mathbf{s} = \boldsymbol{\sigma} - \sigma_m \mathbf{E}, \quad \sigma_T = \frac{1}{2} (\sigma_I + |\sigma_I|)$$

In this notation $\dot{\boldsymbol{\epsilon}}^{cr}$ is the creep strain rate tensor, $\boldsymbol{\sigma}$ is the stress tensor, \mathbf{s} is the stress deviator, σ_{vM} is the von Mises stress, σ_T is the maximum tensile stress, σ_I is the first principal stress, σ_m is the mean stress, \mathbf{E} is the second rank unit tensor and ω is the damage parameter. The weighting factors α and β characterize the influence of the principal damage mechanisms (σ_T -controlled, σ_m -controlled or σ_{vM} -controlled). a , b , n , k and l are material constants, which are determined from creep tests at a constant temperature. The model (1) ignores the effects of primary creep.

As an example of application of equations (1) let us introduce the 316 stainless steel at 650°C with the material constants presented in Liu et al. (1994): $a = 2.13 \cdot 10^{-13} \text{ MPa}^{-n}/\text{h}$, $b = 9 \cdot 10^{-10} \text{ MPa}^{-k}/\text{h}$, $n = 3.5$, $k = l = 2.8$, $\alpha = 1$, $\beta = 0$. The elastic constants are $E = 1.44 \cdot 10^5 \text{ MPa}$ as Young's modulus and $\nu = 0.314$ as Poisson's ratio. Let us illustrate the creep responses according to the constitutive model (1) and consider the following stress tensor

$$\boldsymbol{\sigma} = \sigma \mathbf{m} \otimes \mathbf{m} + \tau (\mathbf{n} \otimes \mathbf{m} + \mathbf{m} \otimes \mathbf{n}), \quad \mathbf{n} \cdot \mathbf{n} = \mathbf{m} \cdot \mathbf{m} = 1, \quad \mathbf{m} \cdot \mathbf{n} = 0 \quad (2)$$

Based on the constitutive model (1) some numerical creep tests resulting in creep strain versus time curves were performed: $\dot{\boldsymbol{\epsilon}}^{cr}(t) = \mathbf{m} \cdot \boldsymbol{\epsilon}^{cr}(t) \cdot \mathbf{m}$ under uniaxial tension $\sigma > 0$, $\tau = 0$; $\dot{\boldsymbol{\epsilon}}^{cr}(t) = 2\mathbf{n} \cdot \boldsymbol{\epsilon}^{cr}(t) \cdot \mathbf{m}$ under uniform shear $\sigma = 0$, $\tau = \sigma/\sqrt{3}$, and $|\dot{\boldsymbol{\epsilon}}^{cr}(t)| = |\mathbf{m} \cdot \boldsymbol{\epsilon}^{cr}(t) \cdot \mathbf{m}|$ under uniaxial compression $\sigma < 0$, $\tau = 0$. The considered stress states and the stress values provide the same secondary creep with the same minimum creep rates. The tertiary creep responses are quite different and depend significantly on the kind of the applied stress state. Such a dependence has been observed in creep tests on tubular specimen Kowalewski (2001). In addition, creep curves for the combined action of the normal positive (negative) stress and the shear stress were calculated. One can observe that even a small superposed shear stress leads to a considerable shear strain response. The shear strain curve depends not only on the value of the applied shear stress, but more significantly on the value of the normal stress. The change of sign of σ leads to the considerable change of the shear strain response. The discussed

¹In Rimrott (1992) instead of the power law the sinh-law was recommended for moderate and low stress values. In addition, a brief overview of the contributions of F.P.J. Rimrott to the creep and plasticity analysis was given.

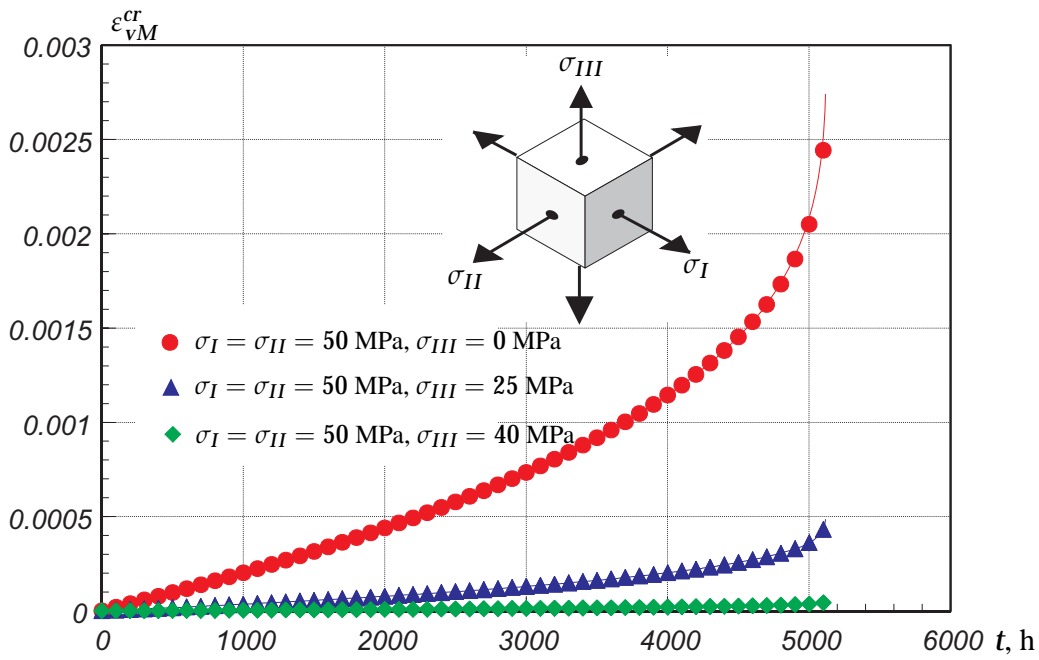


Figure 1. Von Mises Creep Strain vs. Time for Different Stress States

effects can be explained by the dependence of damage mechanisms on the kind of the stress state. A discussion is presented in Naumenko (2000).

Figure 1 shows creep responses under biaxial and triaxial stress states. It can be observed that even a small superposition of the third principal stress significantly reduces the von Mises creep strain rate. For the triaxial stress state with equal principal stresses the model (1) yields the zero equivalent creep strain rate. The fracture time remains unchanged for all stress states presented in Fig. 1 since the damage evolution is controlled by the maximum principal stress. The experimental results on creep-damage under triaxial stress state are discussed in Sakane and Hosokawa (2001).

The stress states with combined action of normal tensile (compressive) stress and small shear stress are typical for transversely loaded beams, plates and shells. For example, the stress state (2) is realized in a beam assuming that \mathbf{m} is the unit vector directed along the beam axis and \mathbf{n} is the unit normal to the beam axis. The creep-damage response of transversely loaded beams is discussed in Altenbach and Naumenko (2002), Naumenko (2000). It was shown that the tertiary creep induces the non-symmetric through the thickness distributions of stresses. The transverse shear strain response cannot be neglected. In addition, the through-the-thickness distribution of the transverse shear stresses differs from the classical parabolic one. Nevertheless, by formulation of suitable constitutive equations for the shear force, the Timoshenko type beam theory can be applied to the creep-damage analysis. In Altenbach et al. (2001) a finite element analysis of a thin-walled pipe bend loaded by internal pressure is performed using the shell and the solid type finite elements. It was shown that in the steady state creep range the shell and the solid elements provide similar predictions. The results for the life-time estimation agree well only in the case of the von Mises equivalent stress σ_{vM} controlled tertiary creep. For the case of the σ_T or σ_m controlled damage evolution the shell and the solid models lead to significantly different results. As will be shown in this paper three-dimensional stress states which are not far from hydrostatic one are possible for moderately thick plates under creep-damage considerations.

3 Equations of Quasi-Static Creep for Moderately Thick Plates

Let us recall the governing equations of the creep mechanics in the classical sense Malinin (1981), Odqvist (1974). For the sake of brevity we consider the geometrically-linear theory, assume isothermal conditions and neglect thermal strains. First, let us consider a three-dimensional deformable body occupying a volume V with the surface A . The body is fixed on the part A_u of A and loaded by a constant traction vector \mathbf{p} on the remaining part A_p . Let $\mathbf{r}(x^i) = \mathbf{e}_i x^i$, $i = 1, 2, 3$ be a vector characterizing the position of the points of the body. The \mathbf{e}_i are basic vectors and the x^i coordinates. The local form of governing equations can be summarized as follows

- Equilibrium conditions

$$\begin{aligned} \nabla \sigma_m + \nabla \cdot \mathbf{s} + \rho \mathbf{f} &= \mathbf{0}, & \mathbf{s}_\times &= \mathbf{0}, \\ \nabla(\dots) &= \mathbf{e}^i \otimes \frac{\partial(\dots)}{\partial x^i}, & (\mathbf{a} \otimes \mathbf{b})_\times &\equiv \mathbf{a} \times \mathbf{b} \end{aligned} \quad (3)$$

- Kinematical equations

$$\begin{aligned} \boldsymbol{\varepsilon} &= \frac{1}{2} \left(\nabla \mathbf{U} + (\nabla \mathbf{U})^T \right) & \Rightarrow & \quad \nabla \times (\nabla \times \boldsymbol{\varepsilon})^T = \mathbf{0}, \\ \boldsymbol{\varepsilon} &= \frac{1}{3} \varepsilon_V \mathbf{E} + \boldsymbol{\varepsilon}, & \varepsilon_V &= \nabla \cdot \mathbf{U} \end{aligned} \quad (4)$$

- Constitutive assumptions

$$\sigma_m = \frac{E}{3(1-2\nu)} \varepsilon_V, \quad \mathbf{s} = 2G(\boldsymbol{\varepsilon} - \boldsymbol{\varepsilon}^{cr}), \quad G = \frac{E}{2(1+\nu)} \quad (5)$$

In equations (3) - (5) the following notations are introduced: $\rho \mathbf{f}$ - the body force vector, \mathbf{U} - the displacement vector, $\boldsymbol{\varepsilon}$ - the tensor of total strains, $\boldsymbol{\varepsilon}$ - its deviatoric part and G - the shear modulus. Note that $\boldsymbol{\varepsilon}^{cr}$ must be calculated from equations (1). As usual we have to prescribe the boundary conditions for the displacement vector $\mathbf{U} = \mathbf{U}_*$ for $x^i \in A_u$ and/or the stress tensor $\boldsymbol{\nu} \cdot \boldsymbol{\sigma} = \mathbf{p}$ for $x^i \in A_p$ with $\boldsymbol{\nu}$ as the outer unit normal. With the constitutive and evolution equations (1) and the initial condition $\boldsymbol{\varepsilon}^{cr}|_{t=0} = \mathbf{0}$, the initial-boundary value problem can be solved numerically by applying a time-step algorithm and a variational method (e.g. the finite element method), see e.g. Zienkiewicz and Taylor (1991).

Various approaches to derive a shell theory have been developed within the assumption of elastic or viscoelastic material behavior. As far as we know, a "closed form" shell theory in the case of creep does not exist at present. The principal problem lies in establishing the constitutive equations of creep with respect to the shell type strain measures i.e. the membrane strains, changes of curvature and transverse shear strains. Although, a general structure of elastic equations can be found based on the direct approach, e.g. Altenbach and Zhilin (1988). The open question is the introduction of appropriate damage measures as well as the identification of damage mechanisms under the shell type stress states, i.e. under pure bending, membrane and transverse shear forces, or their interactions.

In this paper we follow the standard approach which can be summarized as follows:

1. Assume that equations (1), (3) – (5) are applicable to the analysis of creep-damage of a moderately thick solid without any modification.
2. Formulate a variational equation of statics (e.g., based on the principle of virtual displacements) with the known tensor $\boldsymbol{\varepsilon}^{cr}$ for a fixed time (time step).
3. Specify cross-section approximations for the functions to be varied (e.g., the displacement vector \mathbf{U}).
4. Formulate and solve the two-dimensional version of equations (3) – (5).
5. Recover the three-dimensional stress field $\boldsymbol{\sigma}$ from the two-dimensional solution.
6. Insert $\boldsymbol{\sigma}$ into equations (1) in order to calculate the time increments of $\boldsymbol{\varepsilon}^{cr}$ and ω .
7. Update the tensor $\boldsymbol{\varepsilon}^{cr}$ for the next time step and repeat the cycle from step 1.

Depending on the type of the applied variational equation (e.g. displacement type or mixed type) and the type of incorporated cross-section assumptions, different two-dimensional versions of equations (3) – (5) with a different order of complexity can be obtained (i.e. models with forces and moments or models with higher order stress resultants). In the case of linear-elastic plates a huge number of such kind plate theories has been proposed, e.g., Lo et al. (1977), Reddy (1984) and Meenen and Altenbach (2001). Note that the steps 2 and 3 can be performed numerically applying e.g. the Galerkin method to equations (3) – (5). Various types of finite elements which were developed for the inelastic analysis of shells are reviewed in Wriggers (2001). Let us note that if

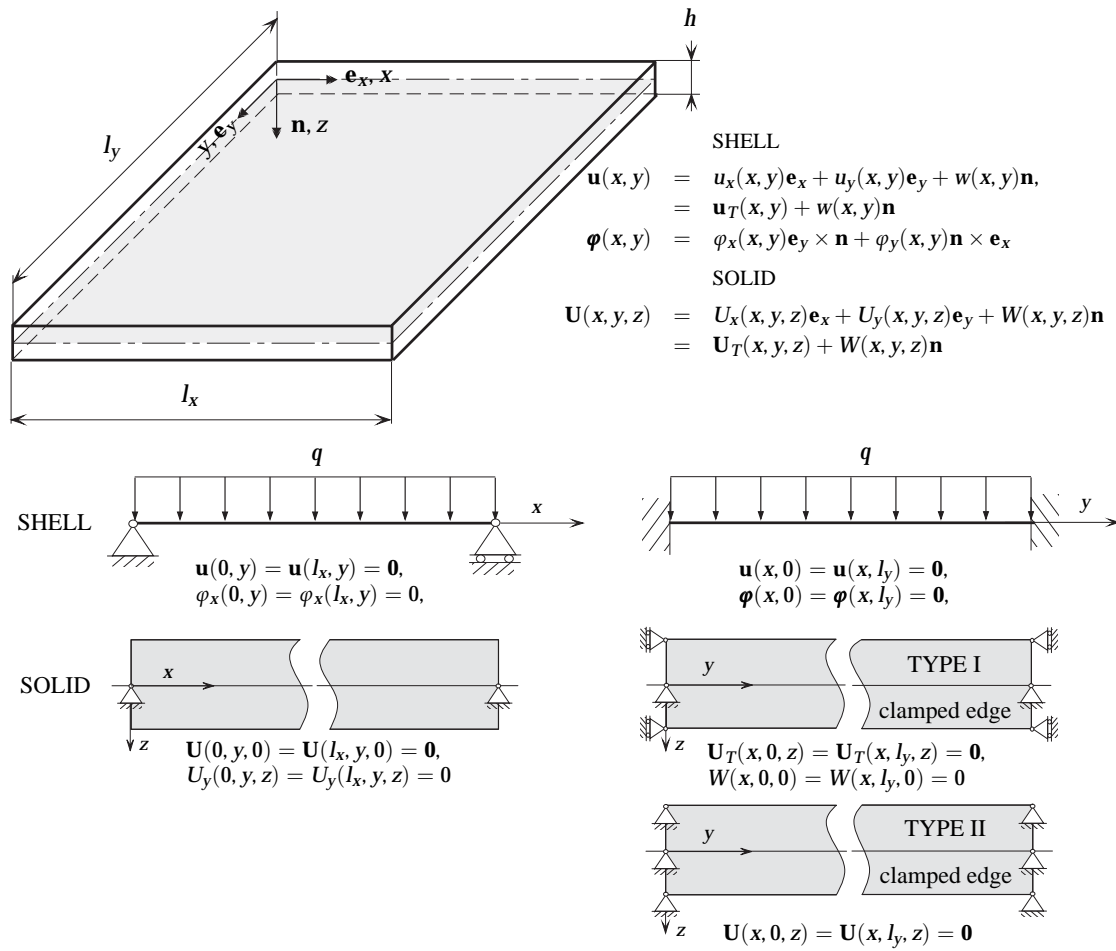


Figure 2. Rectangular Plate: Geometry, Loading and Kinematical Boundary Conditions

studying the creep behavior coupled with damage, the type of assumed cross-section approximations may have a significant influence on the result. For example, if we use a mixed type variational equation and approximate both the displacements and stresses, a parabolic through-the-thickness approximation for the transverse shear stress or a linear approximation for the in-plane stresses is in general not suitable for the creep-damage estimations Altenbach and Naumenko (2002).

4 Numerical Analysis of a Moderately Thick Plate

In order to compare the shell and the three-dimensional models let us perform a finite element analysis of a plate. As an example we selected a moderately thick square plate with $l_x = l_y = 1000$ mm, $h = 100$ mm, loaded by a pressure $q = 2$ MPa uniformly distributed on the top surface, Fig. 2. The edges $x = 0$ and $x = l_x$ are simply supported (hard hinged support) and the edges $y = 0$ and $y = l_y$ are clamped. Note that applying a displacement based finite element method we can prescribe only the kinematical boundary conditions. According to the first order shear deformation plate model we can specify the vectors of midplane displacements $\mathbf{u}(x, y) = \mathbf{u}_T(x, y) + w(x, y)\mathbf{n}$ and cross-section rotations $\varphi(x, y)$ on the lines $x = \text{const}$ or $y = \text{const}$, Fig. 2. Applying such a model and assuming infinitesimal cross-section rotations the displacement vector $\mathbf{U}(x, y, z)$ is usually assumed to be

$$\mathbf{U}(x, y, z) \approx \mathbf{u}(x, y) + z\varphi(x, y) \times \mathbf{n}, \quad \varphi \cdot \mathbf{n} = 0$$

In the case of the three-dimensional model the displacement vector \mathbf{U} can be prescribed on the planes x_c, y, z or x, y_c, z of the plate edges $x = x_c$ or $y = y_c$. Figure 2 illustrates the kinematical boundary conditions used for the shell and the solid models. Let us note that different boundary conditions which correspond to the clamped edge can be specified if we apply the three-dimensional model. Here we discuss two types of the clamped edge

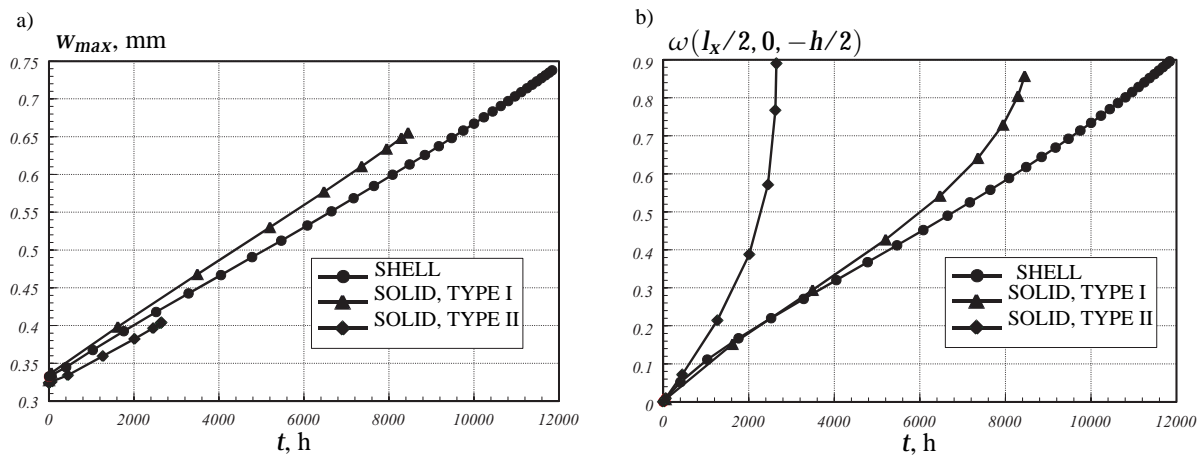


Figure 3. Time Variations: a) Maximum Deflection; b) Damage Parameter

conditions. For the first type (TYPE I), see Fig. 2, we assume the vector of in-plane displacements \mathbf{U}_T to be zero. The deflection W is zero only in the points of the plate mid-surface. In the second type (TYPE II) the whole displacement vector \mathbf{U} is assumed to be zero in all points which belong to the plate edges. The TYPE II boundary condition is the simplest possibility with respect to the effort in the model creation on computer and the preprocessing since all nodal displacements can be simultaneously set to zero on the whole surfaces of the edges $x = \text{const}$ and $y = \text{const}$.

The analysis has been performed using the ANSYS finite element code after incorporating the material model (1) with the help of the user defined creep-damage material subroutine. In Altenbach et al. (2000) we discussed various examples for beams and plates in bending, which verify the modified subroutine. The finite elements available in the ANSYS code for plasticity and creep analysis were used as follows: the 20 nodes solid element SOLID 95 and the 4 nodes shell element SHELL 43. 30×15 elements were used for a half of the plate in the case of the shell model and $30 \times 15 \times 3$ elements in the case of the solid model. The meshes have been justified based on the elasticity solutions and the steady state creep solutions neglecting damage. With these meshes the reference stress distributions as well as the distributions of the von Mises stresses in the steady creep state were approximately the same for both the solid and the shell elements and did not change anymore by further remeshing. The automatical time stepping feature with a minimum time step 0.1 h has been used. For details of the used elements, the material subroutine, the time integration and equilibrium iteration methods used in ANSYS for creep calculations we refer to ANSYS User's Manual Volume I – IV (1994) and Zienkiewicz and Taylor (1991). The time step based calculations were performed up to $\omega = \omega_* = 0.9$, where ω_* is the selected critical value of the damage parameter.

Figure 3 illustrates the results of the computations, where the maximum deflection and the maximum value of the damage parameter are plotted as functions of time. From Fig. 3a we observe that the starting values of maximum deflection as well as the starting rates of the deflection growth due to creep are approximately the same for the shell and the two solid models. Consequently the type of the elements (shell or solid) and the type of the applied boundary conditions in the case of the solid elements has a small influence on the description of the steady-state creep process. However, the three used models lead to quite different life time predictions. The difference can be clearly seen in Fig. 3b. The shell model overestimates the time to failure, while the result based on the solid model depends significantly on the type of the clamped edge boundary conditions. In the case of the TYPE II clamped edge much more accelerated damage growth is obtained. The corresponding time to failure is approximately four times shorter compared to those based on the TYPE I clamped edge. All considered models predict the zone of maximum damage to be in the midpoint of the clamped edge on the plate top surface, as shown in Fig. 4.

The creep response of a structure is connected with the time-dependent stress redistribution, that means the initial elastic stress response changes with time during the creep process. If the applied load and the boundary conditions are assumed to be constant and the effect of tertiary creep is ignored, than an asymptotic stress state exists, which is known as the state of stationary creep Malinin (1981), Odqvist (1974). If tertiary creep is considered, then stresses change with time up to the critical damage state. It is clear that the damage growth and the tertiary creep behavior of the considered plate is controlled by the local stress state in the vicinity of the clamped edges. Figure 5 illustrates the stress states in the midpoint of the clamped edge with the coordinates $x = l_x/2, y = 0$. Four

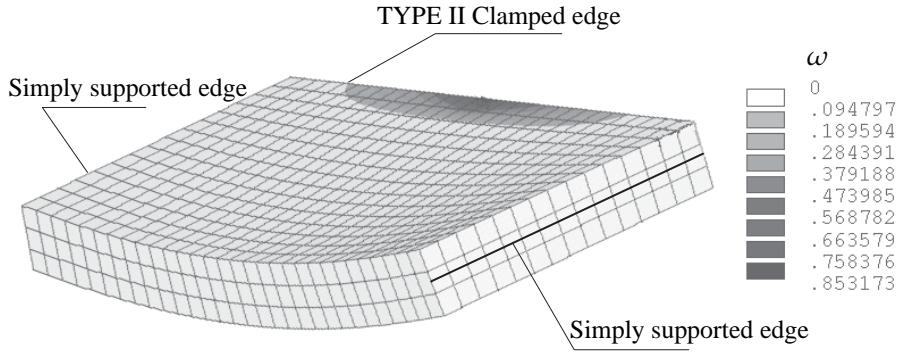


Figure 4. Deformed Shape of a Half of the Plate and Distribution of the Damage Parameter in the Zone of a Clamped Edge (SOLID Elements, TYPE II Boundary Conditions, Last Time Step)

components of the stress tensor (two remaining components are zero due to symmetry conditions) are plotted as functions of the normalized thickness coordinate. The starting elastic distributions (solid lines) as well as the creep solutions at the last time step (dotted lines) are presented. The maximum starting stresses obtained by use of three considered models are the normal in-plane stresses σ_{yy} and σ_{xx} (the stresses which results in the maximum bending and twisting moments in the clamped edge), Fig. 5. These in-plane stresses remain dominant during the whole creep process for the used shell and solid elements. Therefore, all the applied models predict the damage evolution in the zone of the clamped edge on the plate top side. However, the influence of the "second order" stresses (stresses which are usually neglected in the plate theories) is different and depends on the type of the boundary conditions. For the TYPE I clamped edge the effect of the transverse normal stress σ_{zz} decreases with time and has negligible influence on the stress state. In contrast, for the TYPE II clamped edge the initial transverse normal stress σ_{zz} remains approximately constant, while σ_{yy} relaxes with time as the consequence of creep. The transverse normal stress becomes comparable with the bending stress and cannot be considered as the "second order" effect anymore.

In order to explain the difference in life-time predictions let us compare the stress states in the critical zone for the considered models. With respect to the transverse normal and transverse shear stresses the TYPE I and TYPE II boundary conditions lead to different results. For the TYPE I clamped edge the transverse normal stress σ_{zz} has the value of the applied transverse load q on the top plate face and remains constant during the creep process. The transverse shear stress τ_{xz} is zero due to the applied boundary conditions. The stress state on the top side of the plate is primarily determined by two in-plane stresses σ_{xx} and σ_{yy} , Fig. 5. Such a stress state with dominant in-plane stresses and small transverse normal and shear stresses can be obtained applying the first order shear deformation plate theory. In contrast, if applying the TYPE II boundary conditions the results show the considerable value of the transverse normal stress σ_{zz} which remains approximately constant during the creep process.

Now let us estimate the stress state for the TYPE II clamped edge $y = y_c$. In this case we have to set $\mathbf{U}(\mathbf{x}, y_c, z) = \mathbf{0}$ on the plane \mathbf{x}, y_c, z , Fig. 2. For $0 < x < l_x$ and $-h/2 < z < h/2$ we can write

$$\begin{aligned} \frac{\partial \mathbf{U}}{\partial \mathbf{x}} = \frac{\partial \mathbf{U}}{\partial z} = \mathbf{0} & \Rightarrow \nabla \mathbf{U}(\mathbf{x}, y_c, z) = \mathbf{e}_y \otimes \frac{\partial \mathbf{U}}{\partial y}, \\ \text{tr} \boldsymbol{\varepsilon}(\mathbf{x}, y_c, z) = \nabla \cdot \mathbf{U} = \frac{\partial U_y}{\partial y} \end{aligned} \quad (6)$$

In addition, we can set $\mathbf{e}_x \cdot \mathbf{U}(l_x/2, y, z) = \mathbf{0}$ due to the symmetry condition. The starting elastic stress state at $t = 0$ can be obtained from the constitutive equations (5) by setting $\boldsymbol{\varepsilon}^{cr} = \mathbf{0}$

$$\begin{aligned} \sigma_m|_{t=0} &= \frac{1}{3} \frac{1+\nu}{1-2\nu} \sigma_0, & \sigma_0 &= 2G \frac{\partial U_y}{\partial y} \Big|_{t=0}, & \tau_0 &= G \frac{\partial W}{\partial y} \Big|_{t=0}, \\ \mathbf{s}|_{t=0} &= \frac{1}{3} \sigma_0 [2\mathbf{e}_y \otimes \mathbf{e}_y - (\mathbf{E} - \mathbf{e}_y \otimes \mathbf{e}_y)] + \tau_0 (\mathbf{e}_y \otimes \mathbf{n} + \mathbf{n} \otimes \mathbf{e}_y), \\ \boldsymbol{\sigma}|_{t=0} &= \frac{1-\nu}{1-2\nu} \sigma_0 \left[\mathbf{e}_y \otimes \mathbf{e}_y + \frac{\nu}{1-\nu} (\mathbf{E} - \mathbf{e}_y \otimes \mathbf{e}_y) \right] + \tau_0 (\mathbf{e}_y \otimes \mathbf{n} + \mathbf{n} \otimes \mathbf{e}_y) \end{aligned} \quad (7)$$

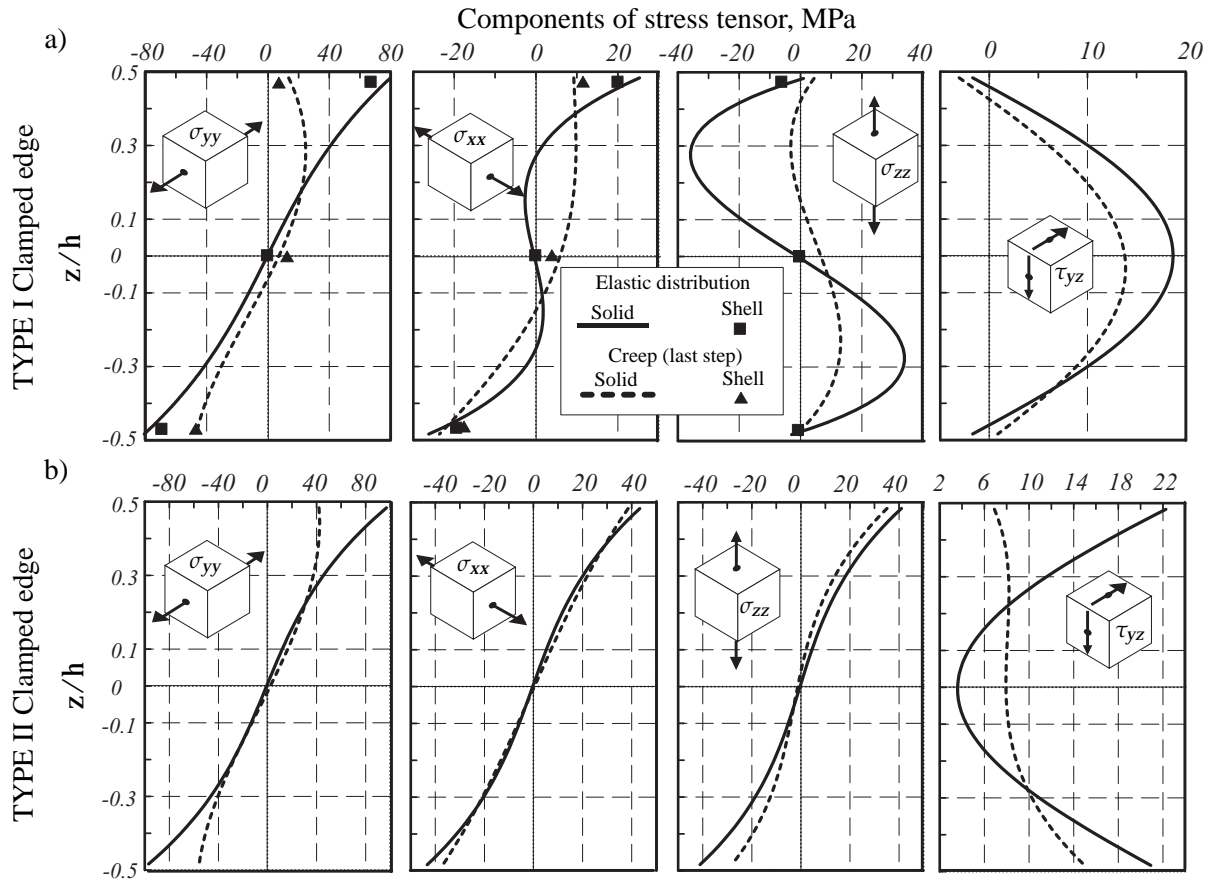


Figure 5. Local Stress State in a Midpoint of the Clamped Edge vs. Thickness Coordinate (Last Time Step):
a) TYPE I Clamped Edge; b) TYPE II Clamped Edge

From the last equation in (7) we see that $\sigma_{zz} = \sigma_{xx} = \sigma_{yy}\nu/(1-\nu)$. This well known result of the linear isotropic elasticity agrees with the obtained finite element solution for $\nu = 0.314$, Fig. 5b (solid lines). Note that within the first order shear deformation plate theory, the transverse normal stress has the order of the applied pressure q .

Let us estimate the stress redistribution in a clamped edge as a consequence of creep. For this purpose we neglect the damage evolution by setting $\omega = 0$ in (1). Because the boundary conditions and the applied pressure are independent of time, we can estimate the type of the stress state under stationary state creep by setting $\dot{\epsilon} \approx \dot{\epsilon}^{cr}$, $\dot{\epsilon}_V \approx 0$ or

$$\frac{1}{2} \left(\mathbf{e}_y \otimes \frac{\partial \dot{\mathbf{U}}}{\partial y} + \frac{\partial \dot{\mathbf{U}}}{\partial y} \otimes \mathbf{e}_y \right) \approx \dot{\epsilon}^{cr} = \frac{3}{2} a \sigma_{vM}^{n-1} \mathbf{s}, \quad \nabla \cdot \dot{\mathbf{U}} \approx 0 \quad (8)$$

Consequently

$$\frac{1}{2} \frac{\partial \dot{W}}{\partial y} (\mathbf{e}_y \otimes \mathbf{n} + \mathbf{n} \otimes \mathbf{e}_y) \approx \frac{3}{2} a \sigma_{vM}^{n-1} \mathbf{s} \quad (9)$$

From equation (9) we observe that the stress deviator in the steady-state creep has the form $\mathbf{s} \approx \tau(\mathbf{e}_y \otimes \mathbf{n} + \mathbf{n} \otimes \mathbf{e}_y)$ and is determined by the transverse shear stress. The mean stress σ_m cannot be determined from the constitutive equation, it must be found from the equilibrium condition (3). The stress state in the zone of the clamped edge $(l_x/2, y, z)$ is then of the type $\boldsymbol{\sigma} \approx \sigma_m \mathbf{E} + \tau(\mathbf{e}_y \otimes \mathbf{n} + \mathbf{n} \otimes \mathbf{e}_y)$. We observe that $\sigma_{zz} \approx \sigma_{yy} \approx \sigma_{xx} \approx \sigma_m$ after the transient stress redistribution. This estimation agrees again with the obtained finite element solution Fig. 5b (dotted lines). The transverse normal stress is approximately equal to the in-plane stresses and cannot be neglected.

Let us compare the finite element results for the mean stress and the von Mises equivalent stress. Figure 6a shows

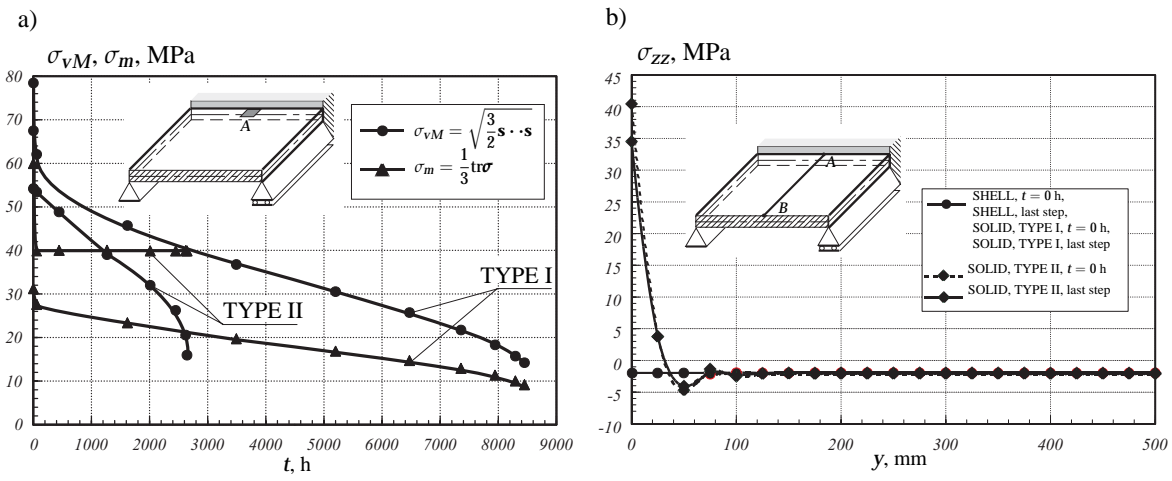


Figure 6. Transversely Loaded Plate: a) von Mises Equivalent Stress and Hydrostatic Stress vs. Time, Element A of the Clamped Edge; b) Transverse Normal Stress σ_{zz} in Elements Along the Line AB;

the corresponding time variations in the element A of the solid model for the TYPE I and TYPE II boundary conditions. We observe that the TYPE II boundary condition leads to a lower starting value of the von Mises stress and a higher starting value of the mean stress when compared with those for the TYPE I boundary condition. In addition, for the TYPE II clamped edge we observe that the mean stress rapidly decreases within the short transition time and after that remains constant while the von Mises stress relaxes during the whole creep process. With the relaxation of σ_{vM} the stress state tends to $\sigma = \sigma_m \mathbf{E}$. The relatively high constant value of σ_m is the reason for the obtained increase of damage and much shorter time to fracture in the case of the TYPE II clamped edge (see Fig. 3b). Note that the above effect of the mean stress has a local character and is observed only in the neighborhood of the edge. As Fig. 6b shows the value of the transverse normal stress decreases rapidly with increased distance from the boundary.

5 Conclusions

We discussed the possibilities of creep-damage behavior modelling in moderately thick structural elements. The selected constitutive model of creep is based on the assumption that the secondary creep strain rate is determined by the deviatoric part of the stress tensor and the von Mises equivalent stress, while the increase of creep rate in the tertiary range is due to isotropic damage evolution which is controlled by the mean stress, the first principal stress and the von Mises equivalent stress. The use of this model in connection with long-term predictions of thin-walled structural elements has motivated a numerical comparative study two approaches: the three-dimensional approach and the approach based on the first order shear deformation type plate theory. The finite element results as well as some simplified estimates have shown that the approaches based on standard solid and shell finite elements provide quite different predictions. The model based on the shell elements overestimates the fracture time. The reason for the obtained differences is the local stress response in the zone of the clamped edge. In the case of linear isotropic elasticity the transverse normal and shear stresses in the zone of the clamped edge can be assumed to be the second order quantities in comparison to the dominant in-plane stresses. In the case of steady state creep, the transverse normal and shear stresses are comparable with the in-plane stresses due to the stress redistribution. If studying the creep behavior coupled with damage, the influence of these factors cannot be ignored.

If a shell or a plate theory is considered to be an approximate version of the three-dimensional equations (3)-(5) then we can conclude that "more accurate" cross-section approximations for the transverse normal and shear stresses have to be used in the case of creep. In this sense it is more reliable to solve the three-dimensional equations (3)-(5) which are "free" from ad hoc assumptions for the displacements and stresses. However, in this case the question about the relevance of "three-dimensional" constitutive assumptions (1) and (5) for the analysis of thin-walled structural elements has to be discussed.

References

- Altenbach, H.; Kolarow, G.; Morachkovsky, O.; Naumenko, K.: On the accuracy of creep-damage predictions in thinwalled structures using the finite element method. *Comp. Mech.*, 25, (2000), 87–98.
- Altenbach, H.; Kushnevsky, V.; Naumenko, K.: On the use of solid and shell type finite elements in creep-damage predictions of thinwalled structures. *Arch. Appl. Mech.*, 71, (2001), 164–181.
- Altenbach, H.; Naumenko, K.: Shear correction factors in creep-damage analysis of beams, plates and shells. *JSME International Journal, Series A*, 45, 1, (2002), 77–83.
- Altenbach, H.; Zhilin, P. A.: Osnovnye uravneniya neklassicheskoi teorii uprugikh obolochek (governing equations of the non-classical theory of elastic shells). *Uspekhi Mekhaniki*, 11, (1988), 107–148.
- El-Magd, E.; Betten, J.; Palmen, P.: Auswirkung der schädigungsanisotropie auf die lebensdauer von stählen bei zeitstandsbeanspruchung. *Mat.-wiss. u. Werkstofftechn.*, 27, (1996), 239 – 245.
- Frost, H. J.; Ashby, M. F.: *Deformation-Mechanism Maps*. Oxford et al.: Pergamon (1982).
- Hayhurst, D. R.: Computational continuum damaged mechanics: its use in the prediction of creep in structures - past, present and future. In: *IUTAM Symposium on Creep in Structures* (edited by Murakami, S.; Ohno, N.), pages 175–188. Dordrecht: Kluwer (2001).
- Kowalewski, Z. L.: Assessment of the multiaxial creep data based on the isochronous creep surface concept. In: *IUTAM Symposium on Creep in Structures* (edited by Murakami, S.; Ohno, N.), pages 401–418. Dordrecht: Kluwer (2001).
- Leckie, F. A.; Hayhurst, D. R.: Constitutive equations for creep rupture. *Acta Metall.*, 25, (1977), 1059 – 1070.
- Liu, Y.; Murakami, S.; Kanagawa, Y.: Mesh-dependence and stress singularity in finite element analysis of creep crack growth by continuum damage mechanics approach. *Eur. J. Mech., A Solids*, 13, 3, (1994), 395–417.
- Lo, K. H.; Christensen, R. M.; Wu, E. M.: A high-order theory of plate deformation. Part I: Homogeneous plates. *Transactions of the American Society of Mechanical Engineers. Journal of Applied Mechanics*, 44, 4, (1977), 663–668.
- Malinin, N. N.: *Raschet na polzuchest' konstrukcionnykh elementov (Creep calculations of structural elements, in Russ.)*. Moskva: Mashinostroenie (1981).
- Meenen, J.; Altenbach, H.: A consistent deduction of von Kármán-type plate theories from threedimensional non-linear continuum mechanics. *Acta Mechanica*, 147, (2001), 1 – 17.
- Naumenko, K.: On the use of the first order shear deformation models of beams, plates and shells in creep lifetime estimations. *Technische Mechanik*, 20, 3, (2000), 215–226.
- Odqvist, F. K. G.: *Mathematical Theory of Creep and Creep Rupture*. Oxford et al.: Oxford University Press (1974).
- ANSYS User's Manual Volume I – IV: *Swanson Analysis Systems, Inc.* (1994).
- Reddy, J. N.: A simple higher-order theory for laminated composite plate. *Trans. ASME. J. Appl. Mech.*, 51, (1984), 745–752.
- Rimrott, F.: On the prediction of the creep life of a thin-walled shaft. *J. Thermal Stresses*, 15, (1992), 101 – 108.
- Sakane, M.; Hosokawa, T.: Biaxial and triaxial creep testing of type 304 stainless steel at 923 k. In: *IUTAM Symposium on Creep in Structures* (edited by Murakami, S.; Ohno, N.), pages 411–418. Dordrecht: Kluwer (2001).
- Wriggers, P.: *Nichtlineare Finite-Element-Methoden*. Berlin u.a.: Springer (2001).
- Zienkiewicz, O. C.; Taylor, R. L.: *The Finite Element Method*. London et al.: McGraw-Hill (1991).

Address: Prof. Dr.-Ing.Dr.h.c. Johannes Altenbach, Förderstedter Str. 28, D-39112 Magdeburg; Prof. Dr.-Ing. Holm Altenbach, Dr.-Ing. Konstantin Naumenko, Fachbereich Ingenieurwissenschaften, Lehrstuhl für Technische Mechanik, Martin-Luther-Universität Halle-Wittenberg, D-06099 Halle.
e-mail: holm.altenbach@iw.uni-halle.de